

PHOTOELECTRON YIELD AND PHOTON REFLECTIVITY FROM CANDIDATE LHC VACUUM CHAMBER MATERIALS WITH IMPLICATIONS TO THE VACUUM CHAMBER DESIGN

V. Baglin, I. R. Collins and O. Gröbner, CERN, Geneva, Switzerland

Abstract

Studies of the photoelectron yield and photon reflectivity at grazing incidence (11 mrad) from candidate LHC vacuum chamber materials have been made on a dedicated beam line on the Electron-Positron Accumulator (EPA) ring at CERN. These measurements provide realistic input toward a better understanding of the electron cloud phenomena expected in the LHC. The measurements were made using synchrotron radiation with critical photon energies of 194 eV and 45 eV; the latter corresponding to that of the LHC at the design energy of 7 TeV. The test materials are mainly copper, either, i) coated by co-lamination or by electroplating onto stainless steel, or ii) bulk copper prepared by special machining. The key parameters explored were the effect of surface roughness on the reflectivity and the photoelectron yield at grazing photon incidence, and the effect of magnetic field direction on the yields measured at normal photon incidence. The implications of the results on the electron cloud phenomena, and thus the LHC vacuum chamber design, is discussed.

1 INTRODUCTION

Intensive studies have been undertaken to estimate the possible effects of an electron-cloud in the LHC causing heat load to the beam screen, beam induced multipacting and an electron-cloud instability [1, 2, 3, 4, 5]. These phenomena are modeled with a number of input parameters, which include the photon reflectivity, R , the electron yield per adsorbed photon, Y^* , the secondary electron yield, δ , and its dependence on energy, and the energy distribution of the emitted electrons. To make more precise estimates, these parameters have been measured for some candidate materials for the LHC vacuum system. Here we present results for Y^* and R at a mean photon incidence angle of 11 mrad.

2 EXPERIMENTAL DETAILS

2.1 Experimental System

An existing beam line on the EPA ring [6] at CERN, used previously for measuring molecular photodesorption yield of Al, Cu and stainless steel materials [7], was used for these studies and is shown in Figure 1. The synchrotron radiation produced by a EPA bending magnet enters the beam line through a square collimator (11x11 mm²) which defines a beam divergence of

± 3.9 mrad. During an experiment a 4.2 m long test chamber is irradiated at a mean incidence angle of 11 mrad over 3.4 m of its length with either 45 eV or 194 eV critical energy synchrotron radiation. Due to the vertical collimation, photon energies below about 4 eV are attenuated.

A machined OFHC Cu collector and a stainless steel wire electrode were mounted in the tested chambers to measure the forward scattered photon reflection and the photoelectron yields respectively.

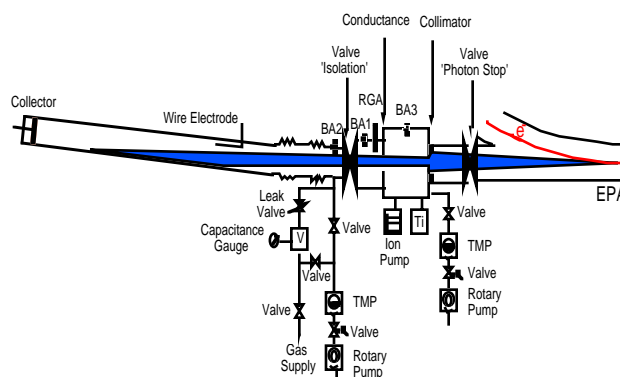


Figure 1. Schematic of EPA beam line

2.2 Test chamber preparation

The studied surfaces were Cu, prepared in the form of liners which could be inserted into a stainless steel chamber. Cu is preferred as it has a high electrical conductivity thus minimising resistive wall effects. These Cu surfaces were studied mainly without bakeout in order to simulate more closely the situation in the LHC. Typical base pressures of a few 10^{-8} Torr were obtained during measurements. The surfaces and their preparation details are given below:

a) 50 μm Cu co-laminated onto a high-Mn content stainless steel and annealed under H_2 at 920°C for 7.5 minutes. An average surface roughness, R_{a} , of 0.2 μm was found using a contactless device (Perthen RM600), while Atomic Force Microscopy (AFM) measurements indicate an average surface roughness of 12 nm over a $8 \times 8 \mu\text{m}^2$ surface area.

b) *Ex-situ* air baking at 350°C for 5 minutes of the aforementioned Cu surface resulting in an average surface roughness of 64 nm from AFM measurements.

c) Cu electro-deposited from a Cu-sulphate bath onto 316LN stainless steel, with an average surface roughness of 1.6 μm measured by the contactless measuring device.

d) A Cu sawtooth structure, 0.5 mm step height and 10 mm periodicity, mounted such that the photons were incident quasi-normal to the vertical face of the sawtooth. This surface was studied in three different surface conditions: as-received, baked at 150°C for 9 hours and baked at 150°C for 24 hours.

3 RESULTS

3.1 Photon reflection

With the test chamber aligned in the ‘straight through position’, *i.e.* photons impinging directly onto the collector, a current, I_{ST} , proportional to the photon flux is recorded for a sufficiently large negative bias (space charge is overcome above $\sim 20V$) as shown in Figure 2. The test chamber is then aligned to a mean incidence angle of 11 mrad and irradiated whilst the photoelectron current is measured at the collector. Under the assumption that the photon spectrum is unchanged on reflection, then this collector current, I_{11} , with the same negative bias is proportional to the forward scattered reflected photon flux. The ratio of I_{11} to I_{ST} then defines the forward scattering photon reflection, R . For positive bias of the collector the small recorded current can be attributed to photoelectrons produced on the test chamber by back-scattered light from the collector.

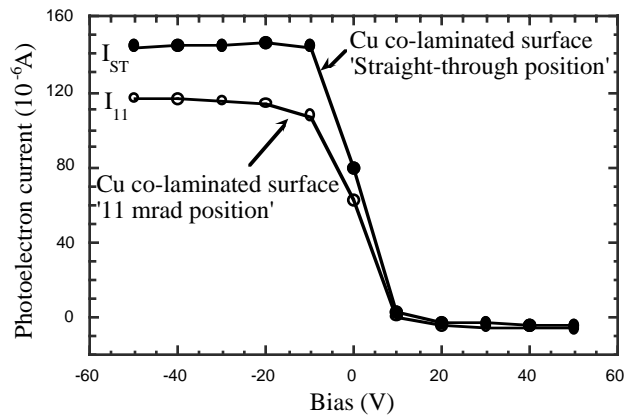


Figure 2. Photoelectron currents, I_{ST} and I_{11} , measured at the collector for the Cu co-laminated test chamber irradiated by 45 eV critical energy synchrotron radiation in straight through and 11 mrad positions respectively.

3.2 Photoelectron yields

The photoelectron yield is measured at the mean angle of incidence of 11 mrad using a positively biased (up to 1kV) 200 mm long stainless steel wire electrode. The measured photocurrent, I_Y , on this electrode converges for increasing voltage but never completely saturates since this measurement is local, *i.e.* the collection length increases with increasing bias. From the measurement of the photoyield of sawtooth chamber with the light at quasi-normal incidence, normalised to the measured photoyield of the end collector at normal incidence, the collection length was determined to be 500 mm.

The electron yield per incident photon, Y , is derived from the photon flux, $\dot{\Gamma}$, into the test chamber making appropriate allowance for the attenuation due to the collimator, F : 46% and 65% of the photons from the beam line enter the set-up at 45 eV and 194 eV critical energies respectively. A correction due to the effective collection length, L_{coll} with respect to the length irradiated, L_{Tr} (3.4 m), is applied. The photoelectron yield is given by: $Y = \frac{I_Y}{q \dot{\Gamma} F} \frac{L_{Tr}}{L_{coll}}$

For the simulations of the electron-cloud and the beam induced multipacting effects, the electron yield per absorbed photon, Y^* , is a more appropriate parameter which is given by: $Y^* = \frac{Y}{1-R}$. A summary of the results for R and Y^* for all materials studied so far is given in Table 1.

Table 1. Forward scattering photon reflection R and photoelectron yields per absorbed photon, Y^* , of the studied materials under different surface conditioning, irradiated by 45 eV and 194 eV critical energy synchrotron radiation.

Surface	Status	45 eV		194 eV	
		R (%)	Y^* (e/ph)	R (%)	Y^* (e/ph)
Cu co-lam.	as-received	80.9	0.114	77.0	0.318
	air baked	21.7	0.096	18.2	0.180
Cu elect.	as-received	5.0	0.084	6.9	0.078
Cu sawtooth	as-received	1.8	0.053	-	-
	150°C, 9h	1.3	0.053	1.2	0.052
	150°C, 24h	1.3	0.040	1.2	0.040

3.3 Effect of magnetic fields on the photoelectron yields

The vacuum system in the arcs of the LHC will be mainly located in strong magnetic fields arising from dipoles, quadrupoles and corrector magnets. In the presence of a magnetic field any emitted electron will be subject to a Lorentz force that can deviate its motion.

For a dipole field (0.08-0.1 T) aligned parallel to the irradiated collector to within $< 0.8^\circ$, a strong suppression, by a factor larger than 50, of the photoelectron yield is observed. The degree of suppression is related to the alignment of the field relative to the emitting surface indicating that the photoelectron emission is non-isotropic; a misalignment of 1.5° results in a suppression factor of 25. The strong suppression is attributed to low energy electrons being turned back into the surface by the external applied field. On the other hand a solenoid field (0.2 T) aligned perpendicular to the surface has no significant effect on the measured photoelectron current, again indicative of a non-isotropic electron emission.

4 DISCUSSION

For a given surface the forward scattered photon reflectivity is slightly higher at 45 eV critical energy than at 194 eV. This observation is in line with the increase of the reflectivity for low photon energies. On the other hand the photoelectron yield seems to increase slightly for increasing critical energy.

The Cu co-laminated material exhibits both the highest forward scattering photon reflection and photoelectron yield, Y^* . *Ex-situ* air baking of this surface reduces significantly the reflection coefficient but has a lesser effect on the photoelectron yield. This air baking has been proposed as a convenient method to form a thick oxide layer which lowers the secondary electron coefficient [8]. As expected, the forward scattering photon reflection and photoelectron yield of the sawtooth chamber is very small, demonstrating that a geometrical solution of the beam screen shape to the electron-cloud and beam induced multipacting is attractive.

5 IMPLICATIONS FOR THE LHC

The primary motivation for this study was to explore the parameters affecting the electron cloud induced heat load which can be improved by an optimised design of the vacuum chamber or beam screen. A preliminary estimate of the heat load and thus of the required cooling capacity of the cryogenic system at the 20 K level has been given in [2] as 0.2 W/m when secondary electrons were not taken into account. More recently, improved computer simulations which include secondary electrons and the magnetic dipole field have been reported in [4, 5]. To apply the results presented here to drift spaces and dipole magnets in the LHC, it is necessary to take into account the observed strong suppression of photoelectrons in the horizontal plane of a dipole magnet and the contribution of reflected photons, which strike top and bottom faces of the beam screen where electrons can be generated. An important condition to be met is that the electron cloud remains in a regime where it is not dominated by the secondary electrons. This assumption implies that the peak of the secondary electron yield, δ_{\max} , is below a critical value, e.g. $\delta_{\max} < 1.3$ for the beam screen in the arc [5]. It is assumed that such a value of δ_{\max} can be obtained by an appropriate surface coating and by conditioning with beam. For the TiN coated vacuum chamber in the PEP II positron ring it is assumed that $\delta_{\max} \sim 1.1$ can be achieved by electron dosing of the surface [9]. In the room temperature parts of the LHC, where most of the vacuum chamber will be baked *in-situ* to guarantee vacuum stability for ion induced desorption, this baking will also reduce δ . In this linear regime, and assuming that the power deposition scales linearly with reflectivity, the computed heat load is given by:

$$P_{\text{dipole}} = f R Y^* P_m,$$

with P_m , the computed linear power load in a dipole magnet and

$$P_{\text{drift}} = Y^* P_o,$$

with P_o , the computed linear power load in a field free region. Here f is a geometrical factor, assumed to be 1/2, accounting for the fact that only those scattered photons which strike the top and bottom faces of the dipole beam screen are effective in producing photoelectrons while photons hitting the inner wall of the beam screen are again suppressed by the dipole field. The result of this linear scaling, based on the data of Table 1 for 45 eV critical energy and [5], is summarised in Table 2.

Table 2. Heat loads for different beam screen and vacuum chamber surfaces. $P_m=4.5$ W/m and $P_o=20$ W/m are taken from [5].

Surface	Status	45 eV		P (W/m)	
		R (%)	Y* (e/ph)	$P_m=4.5$	$P_o=20$
				Dipole	Drift space
Cu co-lam.	as-received	80.9	0.114	0.208	2.28
	air baked	21.7	0.096	0.047	1.92
Cu elect.	as-received	5.0	0.084	0.009	1.68
Cu sawtooth	as-received	1.8	0.053	0.002	1.06
	150°C, 9h	1.3	0.053	0.002	1.06
	150°C, 24h	1.3	0.040	0.001	0.80

The as-received sawtooth solution for the beam screen is a very attractive option since it minimises the heat load corresponding to about 80 % of the allocated cryogenic nominal heat load budget due to the photoelectrons (21.4 W/cell). A different geometrical structure, but so far not investigated, consists of longitudinal grooves along the strip where the photons strike the wall for the purpose of shadowing the top and bottom faces of the beam screen from reflected photons and hence reducing f . Less attractive, and rather difficult in the cold arcs of LHC, are solutions which necessitate *in-situ* bakeout.

6 ACKNOWLEDGMENTS

The assistance of D. Jenson and N. Kos is gratefully acknowledged. We are grateful to J-P. Potier, L. Rinolfi and their operating crew for running the EPA machine at the reduced beam energy to provide the LHC conditions.

REFERENCES

- [1] F. Zimmerman, LHC Project Report 95, 27/2/1997.
- [2] O. Gröbner, LHC Project Report 127, 25/7/1997.
- [3] F. Ruggiero, LHC Project Report 166, 4/2/1998.
- [4] O.S. Brüning, LHC Project Report 158, 7/11/1997.
- [5] M. Furman, LBNL-41482/CBP Note 247, 3/1998 and LHC Project Report 180, 20/5/1998.
- [6] J.P. Potier, L. Rinolfi, these proceedings
- [7] J. Gómez-Goñi, O. Gröbner and A. G. Mathewson, J. Vac. Sci. Technol. **A** 12(4), 1714 (1994).
- [8] I. Bojko, J-L. Dorier, N. Hilleret, C. Scheuerlein, LHC-VAC, Vacuum Technical Note 97-19, 6/1997.
- [9] M.A. Furman, G.R. Lambertson, Proc. PAC 97, Vancouver, 5/1997.